ISBN: 978-3-95450-212-7 ISSN: 2673-5482 doi:10.18429/JACoW-CYCLOTRONS2022-MOPO017

RF CAVITY RESONANT CONTROL USING MINIMAL SEEKING SLIDING MODE CONTROLLER

K. Fong, R. Leewe, T. Au, X. Fu, Q.W. Zheng, TRIUMF, Vancouver, BC, Canada

Abstract

Accelerating RF normal conducting cavities having Quality Factors of over 10^3. These cavities must be constantly tuned to maintain resonance for maximum power efficiency. Traditional tuning method uses 'phase comparison method' by monitoring the phase shift across the input and output of the cavity. This method suffers from phase drift due to diurnal temperature variations. Since 2017, TRIUMF ISAC-1 cavities are tuned using minimal seeking sliding mode controllers, which eliminate effects drift due to temperature changes. As with all extremum seeking algorithm, chattering is present in the system, especially near the end-stage. This paper also includes a new chattering suppression method known as 'surface skipping', which is slated to be installed in ISAC-1 LLRF upgrade in 2023.

INTRODUCTION

In a RF cavity, with $\Delta\omega = \omega - \omega_c$, with ω as the operating frequency, τ the time constant of the cavity and ω_c its resonant frequency, the steady state complex cavity voltage V is given by [1]

$$V \cong \frac{\Gamma+1}{1+(\Delta\omega\tau)^2}(1+j\Delta\omega\tau)v_F \tag{1}$$

where Γ is the reflection coefficient, is the result of impedance matching. Using Kirchhoff's voltage law

$$v_F + v_R = V \tag{2}$$

The reflected voltage v_R is [1]

$$v_r \cong v_f \frac{\Gamma + j\Delta\omega\tau}{1 - j\Delta\omega\tau} \tag{3}$$

The reflected power P_R in relation to the forward power P_F is

$$P_R \cong P_F \frac{\Gamma^2 + (\Delta\omega\tau)^2}{1+(\Delta\omega\tau)^2} \tag{4}$$

and

$$\frac{dP_R}{d(\Delta\omega)} = P_F\left(1-\Gamma^2\right)\tau^2\Delta\omega \tag{5}$$

Minimum P_R occurs when

$$\frac{dP_R}{d(\Delta\omega)} = P_F\left(1-\Gamma^2\right)\tau^2\Delta\omega = 0 \tag{6}$$

or $\Delta\omega = 0$.

From Eq. (1), the phase angle between V and v_F is

$$\phi = \tan^{-1}\Delta\omega\tau \tag{7}$$

At $\Delta\omega = 0$, the RF cavity in will be operating most efficiently. Most cavity do this by applying Eq. (6), monitoring the monotonic ϕ and move the tuner such that $\phi = 0$. However, ϕ cannot be measured in-situ, as there must be some lengths of cables from the input pickup and the output pickup. The lengths of these cables must be carefully matched to prevent phase drift due to diurnal temperature changes. In TRIUMF's ISAC-1, ϕ is measured from the output of the LLRF to the feedback input of the LLRF. This makes the phase measurement even more prone to error due to the rf amplifier chains inherent phase shift dependency on power and temperature. To avoid phase measurement, tuning algorithm in ISAC-1 cavities try to minimize the reflected power P_R instead. From Eq. (4), minimizing v_R or P_R will result in $\Delta\omega \to 0$ and therefore maximizing V. However, as can be seen from Eq. (4) and Fig. 1, P_R is neither linear nor monotonic. This leads us to minimum reflecting power seeking algorithm. There are several minimum seeking algorithms, all of them involve perturbing the system to detect the correct slope to minimization. In gradient estimation minimum seeking algorithm, $\frac{dP_R}{dt}$ is calculated to obtain the direction of travel for the tuner. However, numerical differentiation enhances high frequency noise. The sliding mode extremum seeking algorithm, P_R is used instead to suppress the noise generated by slope detection.

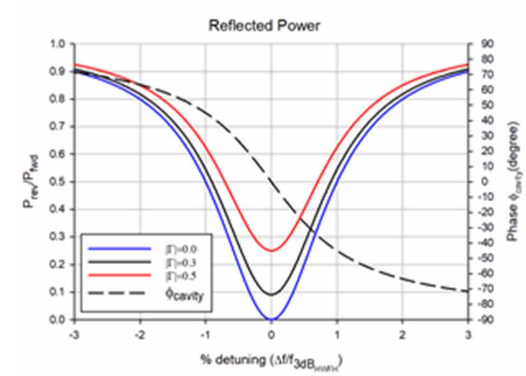

Figure 1. Reflected power vs tuning.

SLIDING MODE EXTREMUM SEEKING ALGORITHM

The original sliding mode equation is given as [2-4]

$$\frac{d\theta}{dt} = k_0 \,\mathrm{sgn}\left[\sin\left(\frac{\pi s}{\varepsilon}\right)\right]F(\theta) \tag{8}$$

ISBN: 978-3-95450-212-7 ISSN: 2673-5482 doi:10.18429/JACoW-CYCLOTRONS2022-MOPO017

with $s(t) = F(\theta) + \rho t$ (9)

A block diagram of a minimum seeking sliding mode controller is shown in Fig. 2.

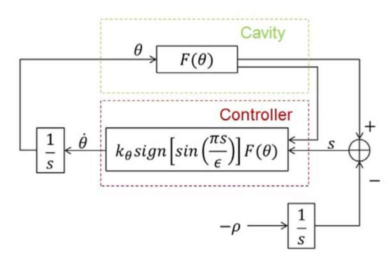

Figure 2. Block diagram of sliding mode controller.

The function to be minimized is $F(\theta) \equiv P_R$, the reflected power, whereas θ is the distance to minimum. ρ, ε and k_0 are tuneable parameters to be optimized for speed of convergence and stability. The sliding mode surfaces are where $s = \varepsilon n$, where $n = 0, \pm 1, \pm 2, \cdots$. For this reason, ε is the separation between the sliding mode surface. As soon as s crosses over one of these surfaces, the movement of the tuner $\frac{d\theta}{dt}$ is reversed. Differentiating Eq. (9) we get

$$\frac{ds}{dt} = \frac{dP_R}{d(\Delta\omega)}\frac{d(\Delta\omega)}{dt} + \rho$$

(10)

and using Eq. (5),

$$\frac{ds}{dt} = P_F\left(1-\Gamma^2\right)\tau^2\frac{1}{2}\left(\frac{d(\Delta\omega)^2}{dt}\right) + \rho$$

(11)

Since P_F, $\left(1-\Gamma^2\right)$, τ and ρ are always positive, $\frac{ds}{dt}$ is smaller when $\left(\frac{d(\Delta\omega)^2}{dt}\right)$ is negative, i.e. $|\Delta\omega| \to 0$.

When $\frac{ds}{dt}$ is small, s remains longer in the same region bounded by two switching surface. Computationally, one can get rid of the sine and sign function in Eq. (8) and simplified and codified as:

```
if ((s %2) >=0 && (s %2)<1) tuner in;
else                          tuner out;
```

The movement is illustrated in Fig. 3 as plots of P_R vs time steps. The green line illustrates idealistic case of the rate of movement completely matches with the decrease in P_R, i.e. $\frac{dP_R}{dt} = -\rho$. The red and blue lines represent more realistic cases when $\frac{dP_R}{dt} \neq -\rho$. When P_R changes slowly compared to ρt the convergence is represent in the blue line, while the red line is when P_R changes rapidly. It shows that in both cases, when P_R is decreasing, the controller stays within this direction longer. However, each time s crosses over a sliding mode surface, the tuner reverses direction, resulting in a sharp increase or decrease in s, causing shorter time in the wrong direction. When P_R reaches the minimum at t=9, the tuner moves back and forth around the minimum point. This end-point chattering can be easily removed by stopping the tuner when P_R falls below a threshold.

SYSTEM PERFORMANCE

In 2016, the resonant controls of ISAC-1's DTL4 and DTL5 were retrofitted with sliding mode controller, and their long-term performances were measured. Fig. 4 shows the performance of the DTL5's sliding mode tuner controller over a period of 4 days in summer of 2016. The purple line is the ambient temperature, clearly showing a diurnal temperature variation of ~10ºC. The red line is the forward power P_F and the purple line is the motor position θ. It is clear from the figure the motor position tracked with the ambient temperature. Within the same time period, there was a setpoint changes as indicated by the jump in P_F as indicated by the red line, which is tracked by the tuner position as well.

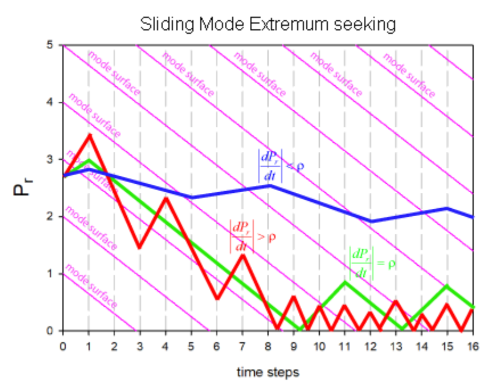

Figure 3. Sliding function dependence on mode surface.

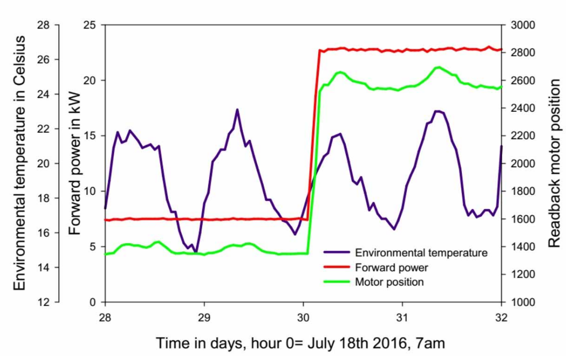

Figure 4. Long term performance of DTL5 in 4 days.

ISBN: 978-3-95450-212-7 ISSN: 2673-5482 doi:10.18429/JACoW-CYCLOTRONS2022-MOPO017

DECHATTERING

As with all extremum seeking algorithm, chattering is present in the system [5-6]. In Fig. 3, the direction of the tuner can switch rapidly, causing a lot of chatter but little overall movement. For example, when the switching function s is close to zero, i.e., from Eqs. (8) and (9)

$$s = P_R + \rho t \approx> 0\ ,\ \frac{dP_R}{dt} + \rho \approx< 0 \text{ and } \frac{dP_R}{dt} < 0\ ,$$

s will drift slowly toward the switch surface $s = 0$. But as soon as $s < 0$, the tuner moves in an opposite direction, causing $\frac{dP_R}{dt} > 0$ and s will arise sharply and back to $s > 0$ and therefore $\frac{dP_R}{dt} < 0$. This process repeats for a while resulting in chatter as illustrated as in both the red and blue curves in Fig. 3. To prevent this from happening, we can add $t \rightarrow t + \Delta t$ to increase s when $s < 0.1$, as well as at other surface boundaries. We call this "switching surface skipping", as it behaves very much like a stone skipping on the surface of water. The following code does this function to every switching function:

```
if (s>-0.1 && s<0) gtime -=  5*Δt;
if (s<0.1 && s>0)  gtime +=  5*Δt;
if (s>0.9)   gtime -=  5*Δt;
if (s<-0.9)   gtime +=  5*Δt;
```

which will set back the value of s to about $0.5 \cdot \Delta t$ as before to eliminate the chatters. This skipping is illustrated in Fig. 5 in a plot of the sliding function vs time. Since skipping changes the values of s but not P_R, the vertical axis is now plotted in s instead of P_R. The blue line is when there is no dechattering and the red line is when dechattering is applied. when the sliding functions get close to a sliding surface, "skipping" cause them to go back to the centre between the two mode surfaces. Since P_R keeps decreasing, P_R would have reached zero at $t \approx 5$ and the controller would enter end-point detection. Figure 6 shows the improvement in convergence when "switching surface skipping" is used as well as end-point detection. In this figure, the blue lines show the movement of a normal sliding mode movement, while the red line show that when the skipping is introduced to make it stay within the same region to prevent a reversal of direction. This also result in a faster convergence as the tuner does not spend time switching direction.

END POINT DETECION

When the minimum is reached, any minimum seeking algorithm will move back and forth around the minimum point and results in further chattering and mechanical wear. To prevent this from happening an endpoint detection must be used, pausing when minimum has been reached. Because the minimum is not necessary equals to zero due to mismatch, so using P_R below a set value is not a good criterion. Instead, the timed average of P_R is used, i.e.,

$$\left\langle \left| \frac{dP_R}{dt} \right| \right\rangle <\approx \varepsilon$$

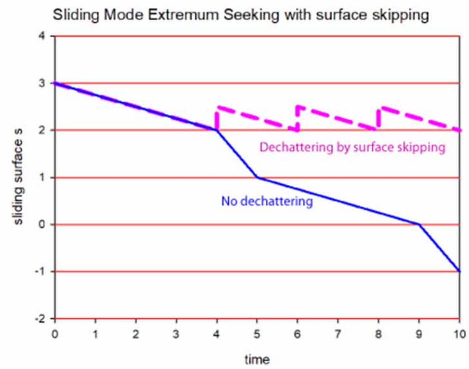

Figure 5. Comparison of sliding mode with and without surface skipping dechattering.

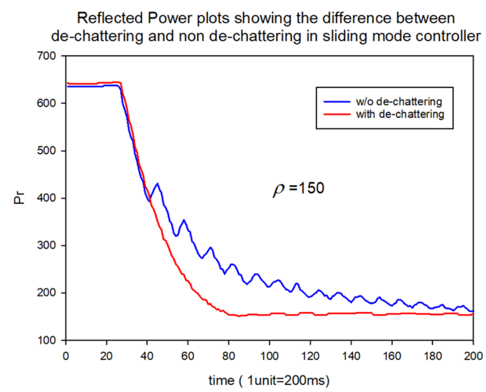

Figure 6. Comparison of reflected power with and without surface skipping dechattering.

to indicate that the end point has been reached. A moving average of 40 samples are used for the averaging, while the differentiation is obtained from coefficients of a Savitzky-Golay filter. The results are shown in Fig. 7, using a $|\Gamma| = 0.3$, where at time=150 the minimum is achieved at about $P_r = 140$. The system continues to switch directions until $\left\langle \left| \frac{d\,P_R}{dt} \right| \right\rangle$ becomes small enough to put the system into hibernation. As can be seen from Fig. 8, there still remains a large amount of chatters before the system finally goes into hibernation. But however this is a small amplitude tuner drive, and the effect on the reflected power is quite small. Nevertheless, in an effort to reduce this chatter, ρ is reduced by a factor of $\frac{1}{2}$ when the reflected power P_R has been reduced to below a pre-set amount closed to

ISBN: 978-3-95450-212-7 ISSN: 2673-5482 doi:10.18429/JACoW-CYCLOTRONS2022-MOPO017

the minimum. But since we cannot reduce ρ without affecting s in Eq. (8), we reduce Δt instead. This is illustrated in Fig. 10. The effect of the reducing of ρ occurs at $t \cong 30$, at which $P_R = 250$. As can be seen in the plot this reduction resulted in a much gentler slope in s. This significantly reduces the amount of chatter and therefore $\left\langle \left| \frac{d\, P_R}{dt} \right| \right\rangle$, allowing the system to go into hibernation much sooner. Furthermore, when the reflected power is below a threshold and $\left\langle \left| \frac{d\, P_R}{dt} \right| \right\rangle > 0$, indicating the power starts to rise again, the system immediately goes into hibernation. These are summarized in the following snippets to reduce Δt. The first part is called "ρ reduction",

```
if ( reversePower < 1.25*slidingMode.dead-band) dtx = 0.5*deltaTime;
if ( reversePower < 1.00*slidingMode.dead-band) dtx = 0.25*deltaTime;
```

and to go into hibernation using the "end detection" :

```
if (fabs(devAvg.val.avg) < 0.5 && rever-sePower < 1.5*slidingMode.deadband) {…}
if (devAvg.val.avg < 1.0 && reversePower < slidingMode.deadband) {…}
if (SGAvgRev.val.der>0 && reversePower < slidingMode.deadband) {…}
```

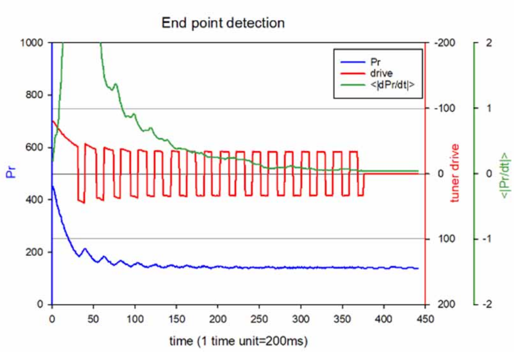

Figure 7. End point (Minimum Reflected power) detection.

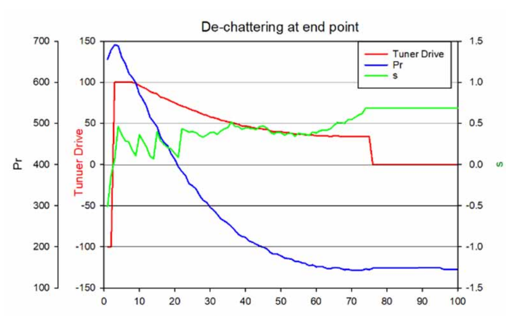

Figure 8. Dechattering at end point by reducing Δt.

However, when the reflected power drops below 250, ρ falls on the correct range and the power reduction is smooth and has a lot less chatter. Conversely for the dechattered case at the mid range the switching is protected by the halo and avoids chattering. However, at $P_R < 300$ the ρ-reduction kicks in and since the original ρ is already too low, the reduced ρ increases the chatter until the "end detection" algorithm kicks in and stop the movement.

CONCLUSION

The position preset, phase alignment and sliding mode controllers will be used in the new ISAC-1 resonance control. Based on each system's strength and weakness, they will be used at different stages of powering up. The position preset mode is used during the initial stage of powering up, when the RF is not yet established and is still in pulse mode. When the RF level reaches a preset value, and switching from pulse to CW is successful, the control enters into phase alignment mode. At this stage the RF will continue to be ramping up. When phase alignment is completed the control will switch to sliding mode. Using a combination of these three modes, the system will benefit from fast ramp-up and resilient to diurnal temperature variations.

REFERENCES

[1] K. Fong, "Beam loading equations", TRIUMF, Vancouver, BC, Canada, Design Note: TRI-DN-13-22, 2013.

[2] R. Leewe, M. Noallem, and K. Fong, "System modeling and control of resonance frequency frequency for an RF cavity using reflected power measurements", in *Proc. 2014 IEEE/ASME Int. Conf. Adv. Intell. Mechantronics*, Besacon, France, Jul. 2014, pp. 703-708. doi:10.1109/AIM.2014.6878161

[3] R. Leewe, "RF Cavity Tuning Based on Reflected Power Measurements", Ph.D. Thesis, Simon Fraser University, Vancouver, BC, Canada, 2017.

[4] R. Leewe, Z. Shahriari, and K.Fong, "Novel Scheme to Tune RF Cavities using Reflected Power", in *Proc. 28th Linear Accelerator Conf. (LINAC'16)*, East Lansing, MI, USA, Sep. 2016, pp. 757-759. doi:10.18429/JACoW-LINAC2016-THOP06

[5] J. Gulder and V. I. Utkin, "The chattering problem in sliding mode systems", in *Proc. 14th Int. Symp. of Mathematical Theory of Networks and Systems"*, Perpignan, France, Jun. 2000. A.E. Jai and M. Fliess, Eds. Université de Perpignan.

[6] H. Lee and V. I. Utkin, "Chattering suppression methods in sliding mode systems", *Annual Reviews in Control*, vol. 32, no 2, pp.179-188, 2007.